

MIMONet: Multi-Input Multi-Output On-Device Deep Learning

Zexin Li¹, Xiaoxi He², Yufei Li¹, Shahab Nikkhoo¹, Wei Yang³, Lothar Thiele⁴, and Cong Liu¹

Abstract—Future intelligent robots are expected to process multiple inputs simultaneously (such as image and audio data) and generate multiple outputs accordingly (such as gender and emotion), similar to humans. Recent research has shown that multi-input single-output (MISO) deep neural networks (DNN) outperform traditional single-input single-output (SISO) models, representing a significant step towards this goal. In this paper, we propose MIMONet, a novel on-device multi-input multi-output (MIMO) DNN framework that achieves high accuracy and on-device efficiency in terms of critical performance metrics such as latency, energy, and memory usage. Leveraging existing SISO model compression techniques, MIMONet develops a new deep-compression method that is specifically tailored to MIMO models. This new method explores unique yet non-trivial properties of the MIMO model, resulting in boosted accuracy and on-device efficiency. Extensive experiments on three embedded platforms commonly used in robotic systems, as well as a case study using the TurtleBot3 robot, demonstrate that MIMONet achieves higher accuracy and superior on-device efficiency compared to state-of-the-art SISO and MISO models, as well as a baseline MIMO model we constructed. Our evaluation highlights the real-world applicability of MIMONet and its potential to significantly enhance the performance of intelligent robotic systems.

I. INTRODUCTION

Single-input single-output (SISO) deep neural networks (DNNs) have demonstrated impressive performance in various robotics applications [1, 2, 3, 4]. However, multi-input single-output (MISO) DNNs have emerged as a promising alternative, as they have been shown to surpass SISO DNNs both theoretically and empirically [5, 6, 7, 8]. Developing MISO DNNs is a crucial step towards creating multi-input multi-output (MIMO) DNNs for intelligent embedded systems, especially in the field of robotics.

In order to create truly intelligent robots, they should be capable of processing a person’s spoken language and facial expressions in real-time and provide tailored feedback based on factors such as gender and emotion. Interactive companion robots, like the Vector Robot [9], are expected to receive camera and microphone inputs and use this information to predict user preferences and respond appropriately. In on-device learning scenarios with strict hardware constraints and performance requirements, deploying multi-input multi-output (MIMO) deep neural networks (DNNs) can be advantageous. By reducing the need to deploy multiple single-input single-output (MISO) DNN instances on the device, MIMO DNNs can significantly lower resource demands. This paper presents MIMONet, a novel on-device

MIMO DNN framework that achieves both high accuracy and on-device efficiency in terms of critical performance metrics including latency, energy, and memory usage. We first constructed a baseline MIMO DNN model and observed that it requires high memory consumption and struggles to meet real-time constraints due to computational demand. To minimize resource demands, MIMONet builds on an existing DNN model compression technique, VIB [10], which is effective for single-input single-output (SISO) DNN models. However, extending VIB to MIMO DNN models posed two new challenges. First, VIB exclusively supports the compression of feed-forward networks [11], which makes it unsuitable for more advanced networks, such as ResNet [12]. To address this limitation, MIMONet extends and develops a modified compression method for ResNet with residual blocks. Second, VIB was not designed to handle MIMO scenarios and did not account for the unique characteristics of MIMO models. VIB focuses on reducing intra-model redundancy but is unable to address common inter-model redundancy in MIMO models. To address this issue, MIMONet develops a new deep-compression method that reduces both inter- and intra-model redundancy, resulting in deeper lossless compression for MIMO scenarios.

We present a two-fold evaluation of MIMONet to demonstrate its accuracy and on-device efficiency. In the first set of experiments, we evaluated the accuracy of MIMONet by comparing it to state-of-the-art SISO and MISO models, as well as a baseline MIMO model, using the RAVDESS multimodal dataset [13]. Our results show that MIMONet consistently outperforms SISO, MISO, and the baseline MIMO model in terms of accuracy, achieving improvements of 13.1%, 2.2%, and 1.0%, respectively. The superiority of MIMONet’s performance is attributed to its deep-compression method, which reduces both inter- and intra-model redundancy in MIMO settings, resulting in deeper lossless compression. In the second set of experiments, we conducted an extensive evaluation of MIMONet’s on-device efficiency in terms of latency, energy, and memory usage. We deployed MIMONet on three widely used embedded system platforms: NVIDIA Jetson Nano, NVIDIA Jetson TX2, and NVIDIA AGX Xavier, which are popular platforms for various robotics applications [1, 2, 3, 14] such as Duckiebot [15], SparkFun Jetbot [16], and Waveshare Jetbot [17]. In addition, we evaluated MIMONet on a PC machine for a more comprehensive assessment. In summary, experimental results demonstrate that MIMONet can achieve:

- **Reduced Memory Usage:** MIMONet significantly reduces runtime memory usage by 31.0% compared to the

¹Authors are with the University of California, Riverside.

²Authors are with the University of Macau.

³Authors are with the University of Texas at Dallas.

⁴Authors are with the ETH Zurich.

baseline Multiple-Input Multiple-Output (MIMO) model.

- **Improved Inference Speed:** MIMONet exhibits speed-ups of 1.44x, 1.80x, 5.64x, and 3.13x compared to the baseline MIMO model when tested on Nano, AGX, TX2, and PC, respectively.
- **Enhanced Energy Efficiency:** The energy savings offered by MIMONet are 1.69x, 1.90x, and 5.18x compared to the baseline MIMO model when tested on Nano, AGX, and TX2, respectively.

In addition to our two-fold evaluation, we conducted a realistic case study using the TurtleBot3 robot to demonstrate the real-world applicability of our proposed approach. Specifically, we evaluated scenarios involving face and audio recognition for interactive emotional robots in a cluttered environment. The results of this case study further validate the superiority of our proposed MIMO model over state-of-the-art SISO and MISO models in terms of accuracy and on-device efficiency. Moreover, we provide visual demonstrations to highlight the effectiveness of our approach in real-world scenarios, demonstrating its practical relevance for interactive robotic systems.

Our contributions can be summarized as follows:

- **Innovative MIMO Framework for robotics:** To the best of our knowledge, MIMONet is one of the first frameworks that utilizes a unified neural network to process multiple inputs and produce multiple outputs simultaneously. This framework is designed to address the intricate inference tasks that are crucial in the context of robotics scenarios.
- **New Deep-Compression Method:** MIMONet introduces a new deep-compression method tailored to enhance the accuracy and on-device efficiency of MIMO framework for robotic applications.
- **Extensive Experimental Results:** Our experiments on three embedded platforms and one PC platform demonstrate that MIMONet achieves high accuracy while delivering superior on-device efficiency in terms of latency, energy, and memory usage. These features make MIMONet an appealing choice for many practical on-device learning scenarios, notably for robots that operate under stringent hardware and performance constraints.

II. BACKGROUND AND RELATED WORK

A. MIMO Model

Current multimodal methods that jointly solve different tasks across domains using a shared model are limited to processing only one task or modality at a time, mostly employing multi-input single-output (MISO) [5, 7, 8] or single-input single-output (SISO) [1, 2, 3, 4] architectures that are difficult to compress and may cause memory and energy consumption issues when used in on-device embedded systems. Existing state-of-the-art models such as BEiT-3 [5], Gato [7], and UniT [8] are examples of such models. On the other hand, concurrent multi-input multi-output (MIMO) works in the field include UniAD [18] and BEVFusion [19], which propose state-of-the-art solutions

for multiple autonomous driving tasks and multi-task multi-sensor fusion, respectively. However, these methods have significant memory and computation resource requirements, and BEVFusion addresses performance bottlenecks by proposing an efficient Bird’s Eye View (BEV) pooling strategy for sensors. To address these challenges, our work focuses on compressing models to ensure real-world deployability.

B. Model Compression for On-device Scenarios

Renowned for their computational and memory requirements, modern DNNs, like the VGG-16 with over 130M parameters, can strain resource-constrained devices during inference in MIMO applications [20]. Model compression methods, which reduce the parameter count without affecting accuracy, offer a solution. They can involve removing redundant parameters [10, 21, 22, 23, 24] or minimizing redundant precision [25]. Two subclasses of model compression exist: single-model pruning and cross-model compression. The former compresses a single network by eliminating unnecessary operations and parameters, while the latter minimizes inter-model redundancy by identifying and removing shared parameters and operations across models [22, 23, 10, 26, 20, 21, 27, 28]. Notably, the Multi-Task Zipping (MTZ) approach has pioneered in cross-model compression by automating the merging of pre-trained DNNs [21]. This study leverages the Variational Information Bottleneck (VIB) method, extending it for application to ResNet architecture. It further modifies MTZ to significantly decrease the total parameters in the proposed MIMO model.

III. METHODOLOGY

A. MIMONet Overview

Fig. 1 illustrates an overview of the on-device MIMO inference framework. First, we train a deep neural network with multiple inputs and multiple outputs (MIMO) as our baseline model (as shown in the first block). One forward prediction of this network requires multiple inputs (image and speech) and generates multiple prediction outputs (emotion and gender) simultaneously.

However, directly deploying such baseline MIMO models to embedded devices remains challenging. Specifically, embedded devices including most robots have *limited memory* and require *real-time performance* for many real-scenario requirements. For instance, handling streaming data (e.g. high-speed cameras sampling 60 times per second) and to ensure robustness in safe-critical scenarios (e.g., autonomous driving robots [15, 29, 30]). In addition, *energy savings* are particularly needed for embedded devices because of limited battery capacity and heat dissipation.

To address these challenges, employing model compression is an intuitive and effective direction. First, we perform single-model compression by adopting the idea of VIB [10] to perform channel-wise hard masking (the masked channel generates zero output while the unmasked channel’s output remains the same). Then, the pruned MIMO model can maintain the original structure in the forward direction. However, VIB is designed for the SISO model and thus

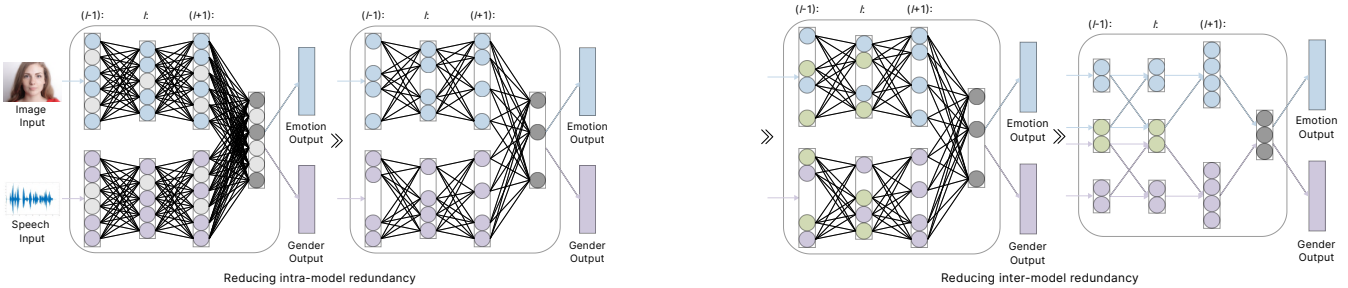


Fig. 1: Overview of MIMONet. In the left part, gray circles represent neurons inducing intra-model redundancy. In the right part, green circles denote sharable neurons inducing inter-model redundancy. Best viewed in color.

reduces the intra-model redundancy. However, it does not consider the characteristics of the MIMO framework, for instance, the MIMO framework is naturally multi-branching and exists inter-model redundancy. Therefore, aiming to reduce such redundancy intuitively can boost model compression performance. Furthermore, inspired by the idea from one cross-model compression work MTZ [21], we perform weights merging between multiple independent branches to improve model compression efficacy further. In summary, in MIMONet we focus on both intra-model redundancy and inter-model redundancy, and thus can theoretically further improve the compression effectiveness and achieve efficient on-device deployment.

B. Reduce Intra-model Redundancy

We aim to reduce intra-model redundancy by performing single-model compression. Specifically, we adopt and extend the idea from VIB [10] that reduces the redundant mutual information between adjacent layers within the model. The vanilla VIB only applies to feedforward neural networks such as VGG [31]. However, for a non-feedforward neural network, e.g., ResNet [12] used in our baseline MIMO model, vanilla VIB is not directly applicable.

Intuitively, we implement VIB by inserting a learnable mask (information bottleneck) between each layer with learnable parameters (convolution layer or fully connected layer). As shown in the left part of Fig. 1, neurons with gray color are masked. Furthermore, combining the characteristics of ResNet, we designed the following adaption scheme: (1) Module-level design: we add the information bottleneck layer as in the original VIB design for the layers not in the residual block. However, we keep the input/output channel number unchanged for each residual block, i.e., we do not insert an information bottleneck layer between two residual blocks. (2) Block-level design: After the second information bottleneck layer, we insert a *channel-recover* operation. This operation restores the channel to the pre-pruning mask based on the pruning mask by filling pruned channels with zeros, which ensures that the input channel is matched during the concatenation operation between the main branch and the bypass. Inspired by the design idea of ResNet [12], we intuitively assume the major information throughout the network is concentrated in the bypass (consisting of direct input or input after downsampling). Therefore, we do not set the mask in the bypass section.

For illustration, we show an example of a basic block of

ResNet in Fig. 2. Surprisingly, as shown in Tab. I, we find that with our design, certain information bottlenecks within the residual block even naturally masked all the output channels (100.0% layer-wise compression rate) from the previous layers when a high compression rate was achieved. This finding verifies our assumption that the main information of ResNet is concentrated in bypass, thus validating the effectiveness of our method.

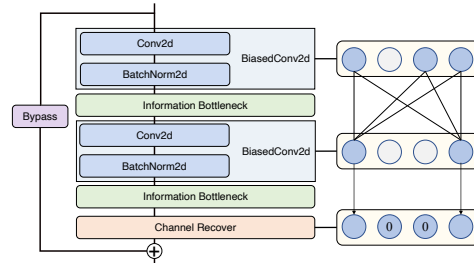


Fig. 2: Design for compression of the residual block for ResNet [12]. The left side shows the structure of the residual block. The right side shows channel-level pruning and recovery. Blue, and gray circles exhibit kept/pruned channels. The pruned channels are filled with zeros before the feature map summing. Best viewed in color.

TABLE I: An example of top-5 layer-wise compression statistics for VIB extension for the baseline MIMO model.

Image	100.0	98.4	97.9	96.1	87.1
Speech	100.0	100.0	99.4	92.2	86.7

Furthermore, we add performance optimization in the residual block to collapse each convolutional (Conv2d) layer and the subsequent batch normalization (BatchNorm2d) layer into a biased convolutional (BiasedConv2d) layer, as shown in the blue box in Fig. 2. Since the on-device deployed models mainly only require forward inference, i.e., all parameters are fixed. Therefore, we could treat the BN layer as an affine transformation and replace it with multiplication and addition. Specifically, the output of the BN layer applied on the i -th channel of layer l is:

$$BN(y_{l,i}) = \gamma_{l,i} \cdot \frac{y_{l,i} - \mu_{l,i}}{\sqrt{\sigma_{l,i}^2 + \epsilon}} + \beta_{l,i} \quad (1)$$

where $y_{l,i}$ is the pre-activation output of the CONV layer, $\gamma_{l,i}$ and $\beta_{l,i}$ are the two learnable parameters (scaling and shifting) for the BN layer, $\mu_{l,i}$ and $\sigma_{l,i}$ are the pre-calculated mean and standard deviation. The effect of the BN layer can

be replaced by multiplying the incoming weight of convolutional layer $w_{l,i}$ by a scalar $\frac{\gamma_{l,i}}{\sigma_{l,i}}$ and adding $\beta_{l,i} - \frac{\gamma_{l,i} \cdot \mu_{l,i}}{\sigma_{l,i}}$ to the bias $b_{l,i}$.

C. Reduce Inter-model Redundancy

After reducing intra-model redundancy, we explore the possibility of decreasing the total number of parameters by reducing the inter-model redundancy through cross-model compression techniques. In a MIMO model, it is not obvious that sharable knowledge exists between the network’s branched parts, as they are processing inputs from an entirely different domain, e.g., one for audio and the other for video input. However, as shown in [32], sharable knowledge still exists within models designed for different input domains, as long as their outputs are fused and serve the same output tasks. Specifically, we have observed a significant amount of sharable knowledge can be found within the later layers, as features are becoming more abstract at this stage, and these abstract features are used for the same tasks.

To this end, we extend the MTZ [21, 32] framework to merge model weights from multiple independent branches. MTZ is a framework that automatically and adaptively merges deep neural networks for cross-model compression via neuron sharing. It calculates the optimal pairs of neurons for sharing in each layer and adjusts their incoming weights, inducing minimal errors. Motivated by this principle, we treat each branch as independent computing sub-graphs in our MIMO model. As shown in the right part of Fig. 1, neurons with green color are shared between different branches. The branches are aligned from the very first layer such that they can be merged and optimized by MTZ layer after layer. This design can also deal with branched layers with different widths, as long as they share the same underlying structure, such as convolutional layers or residual blocks. As proved by experiments, reducing inter-model redundancy effectively reduces the baseline MIMO model size for more efficient on-device deployment.

IV. EVALUATION

A. Experimental Setup

1) *Baselines and Dataset:* We set up four baselines, i.e., a SISO model, a MISO model, a baseline MIMO model, and a VIB-enhanced MIMO model (i.e., applying VIB to the baseline MIMO model). For the SISO model, we use one ResNet-18 as the backbone. For the MISO model, we use a ResNet-18 as the backbone to extract features for each input (image and audio) and concatenate features, followed by three fully connected layers to fuse features and generate multiple prediction results (emotion and gender). For the baseline MIMO model, we design the loss function as a weighted sum of cross entropy losses for each task and use the same model structure as the MISO model.

We choose the Ryerson Audio-Visual Database of Emotional Speech and Song (RAVDESS) dataset [13] to evaluate our proposed method. There are 7356 video files in the RAVDESS (total size: 24.8 GB), among which 24 professional actors, 12 male, and 12 female, are recorded in the

database vocalizing two sentences that are lexically similar in a neutral North American accent. Therefore, this dataset is suitable for MIMO scenarios. Specifically, our MIMO model receives images and audio as inputs and generates emotion prediction together with gender prediction as outputs. As shown before, the emotion and gender prediction outputs can be utilized to develop interactive robots that can interpret and respond to human emotions and gender in a more personalized and natural way. We show some example data in Fig. 3 to illustrate the tasks corresponding to this dataset.

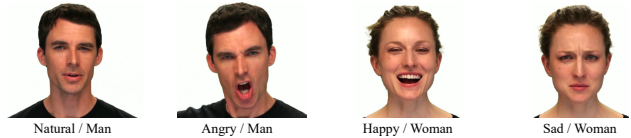


Fig. 3: Data examples of RAVDESS dataset [13].

2) *Implementation Details:* For the SISO model, MISO model, and the baseline MIMO model, we set the learning rate to $1e-4$ for Adam optimizer [33] and train 2000 epochs to ensure the stability and convergence of the training. All models in this paper are trained from scratch for fair comparisons and to eliminate the impact of additional data. For the implementation of VIB [10], we adjust the original parameters of VIB to scale the two subsets of the weighted loss values into the same order of magnitude, thus achieving a better balance of compression rate and accuracy. Specifically, we select the Adam optimizer with a weight decay rate of $5e-5$ and set the learning rate to $1e-3$, IB learning rate to $1e-3$, and KL parameter to $1e-7$. For MTZ, we set merge degree to 0.9 as default in [21]. All of our implementations are based on PyTorch [34]. We measure system-level performance metrics on NVIDIA embedded devices by Tegrastats [35].

3) *Hardware Setup:* We train all DNNs on a server with an Intel E5-2650 CPU and a GeForce RTX 2080 Ti GPU. We conduct inference experiments on an x86-based PC with an Intel i7-10700K CPU and arm-based embedded devices. For embedded devices, we use NVIDIA Jetson Developer Kits (Nano, AGX Xavier, and TX2) ¹, which are widely used as the mainboard of various robots, e.g., Duckiebot [15], SparkFun Jetbot [16], Waveshare Jetbot [17], etc.

B. Metrics

We study the following five metrics to evaluate the accuracy and on-device efficiency of MIMONet. 1) Accuracy: the ratio of correctly identified samples in the test set to the total number of samples in the test set. 2) Parameter number: number of learnable parameters. 3) Memory: required runtime memory for models. 4) Latency: average CPU time required to perform one forward prediction. 5) Energy: We measure system-wide energy consumption. For a fair comparison, we calculate the average energy consumption for each forward inference. We aim to improve on-device efficiency (reduce parameter number, latency, memory, and

¹NVIDIA embedded devices use unified memory, which can introduce large biases in metrics executed on the GPU due to differences in data transfer cost. To ensure fair comparisons, all inferences are running on CPU.

TABLE II: Experimental results of MIMO model’s effectiveness.

Method	Accuracy	Par.($\times 10^6$)	Mem.($\times 10^6$)MB	Latency(ms)				Energy(J)		
				Nano	AGX	TX2	PC	Nano	AGX	TX2
SISO	62.45	11.82	1003.49	329.71	100.57	303.48	4.12	1.12	1.32	1.59
MISO	73.22	25.51	1362.10	412.17	150.23	900.20	16.02	1.58	2.03	4.69
MIMO	74.26	25.51	1364.20	416.01	147.58	905.57	16.91	1.59	2.03	4.71

TABLE III: Ablation study results of accuracy and on-device efficiency.

Method	Accuracy	Par.($\times 10^6$)	Mem.($\times 10^6$)MB	Latency(ms)				Energy(J)		
				Nano	AGX	TX2	PC	Nano	AGX	TX2
MIMO	74.26	25.51	1364.20	416.01	147.58	905.57	16.91	1.59	2.03	4.71
+VIB	76.29	1.07	930.09	226.97	80.54	173.64	6.98	0.75	1.04	0.94
+MTZ	75.51	0.92	940.57	289.18	82.06	160.57	5.40	0.94	1.07	0.91

energy) as much as possible while maintaining the model’s effectiveness (accuracy).

C. Effectiveness of MIMO

Table II illustrates the effectiveness of the proposed MIMO model from multiple perspectives. Firstly, it can be observed that the MISO model achieves significantly higher accuracy (10.8% higher) than the Single-Input Single-Output (SISO) model. This finding demonstrates that utilizing information from multiple inputs can significantly improve the model’s effectiveness. Secondly, our baseline MIMO model demonstrates a slightly higher accuracy (1.0%) than the MISO model, indicating the effectiveness and feasibility of our baseline MIMO framework. By rationally designing this framework, we enhanced the model’s accuracy. On the other hand, MIMO improves on-device efficiency in inference scenarios by reducing memory overhead and computation costs. Specifically, in our task scenario, MISO requires two passes of forward inference to obtain results consistent with MIMO. However, MIMO achieves the same results with only marginally higher memory, latency, and energy consumption than a single forward inference of MISO.

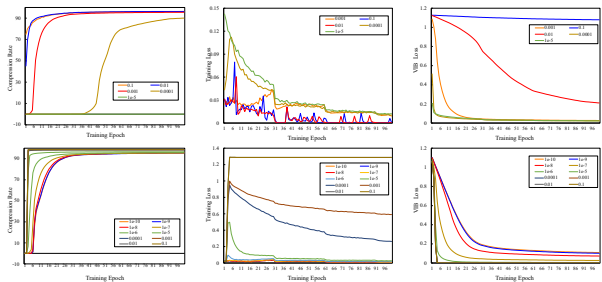


Fig. 4: Parameter study results exhibiting the training curves in reducing intra-model compression.

D. Ablation Study

We show the ablation study results in Table III. We interpret the results in the following two folds:

1) Accuracy: We measure the effectiveness of models by accuracy. It can be observed that applying the extension of VIB and MTZ has almost no degradation in accuracy compared to the baseline MIMO model, outperforming the baseline MIMO model by 2.0% and 1.0%, respectively.

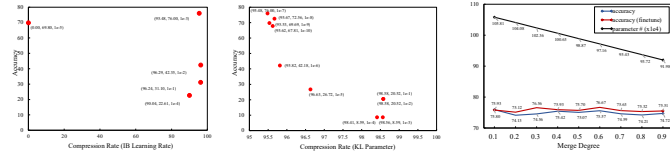


Fig. 5: Parameter study results demonstrating the effect of hyperparameters in our algorithm. The first two figures show the relationships between compression rate and accuracy for the intra-model compression, and the third figure shows the parameter study for the inter-model compression.

This demonstrates that our MIMONet can conduct approximately lossless compression without sacrificing accuracy. This demonstrates that our MIMONet can conduct approximately lossless compression without sacrificing accuracy.

2) On-device efficiency: We measure on-device efficiency by parameter number, memory, latency, and energy.

- Parameter number: Firstly, the experimental results demonstrate that our VIB extension can significantly reduce the parameter number by 95.8% compared to our baseline MIMO model. These experimental results show that our single-model compression method yields outstanding performance in the compression of MIMO models. Furthermore, our proposed MIMONet can reduce the parameter number by 14.0% on top of the VIB extension, reaching 96.4% overall compression rate compared to the baseline MIMO model. These results demonstrate that optimizing the MIMO network structure for internal characteristics (multi-branching) can reduce cross-model redundancy and thus further improve compression performance.
- Memory: In our experiments, we measure runtime memory as one metric to reflect on-device efficiency. It can be observed that MIMONet significantly reduces runtime memory use by 31.1% compared to the MIMO model. Surprisingly, the MIMO model after compression (VIB extension or MIMONet) requires even less runtime memory than the SISO model (as shown in Table II). These results demonstrate our solution’s superiority for on-device deployments, especially for devices with limited memory. For instance, NVIDIA Jetson Nano has only 2 GB runtime memory without enabling swap memory. The limited memory indicates that for SISO, MISO, and

baseline MIMO models, only one instance can be deployed on Nano. In contrast, two instances of MIMONet can be deployed on Nano simultaneously.

- **Latency:** With adding each component of our proposed MIMONet, latency performance gets significantly improved under all other scenarios over the baseline MIMO model. Specifically, MIMONet speed ups the baseline MIMO model by 1.44x, 1.80x, and 5.64x, 3.13x on Nano, AGX, TX2, and PC. It is worth noting that our proposed solutions perform better than the baseline MIMO model on cross-platform hardware. For instance, on the NVIDIA Jetson TX2, the baseline MIMO model requires an average of 905.57 milliseconds to perform a single forward inference, while our proposed MIMONet achieves the same result in just 160.57 milliseconds (5.64x speed-up). On an x86-64 PC, the baseline MIMO model requires an average of 16.91 milliseconds to perform a single forward inference, while our proposed MIMONet achieves the same result in just 5.40 milliseconds (3.13x speed-up).
- **Energy:** MIMONet embodies superiority in energy saving. Specifically, MIMONet has 1.69x, 1.90x, and 5.18x energy saving than the baseline MIMO on Nano, AGX, and TX2, respectively. Furthermore, compared to SISO/MISO models that only generate one output per forwarding inference, our MIMONet framework produces multiple outputs in one forward inference, equivalent to performing multiple inferences by SISO/MISO models. For instance, on AGX, two forward inferences for the MISO model to generate two outputs consume 4.06 joules, while MIMONet generates two outputs consume 1.07 joules (3.79x energy saving).

Efficient on-device deployment: our experimental results demonstrate that MIMONet can address all challenges in Sec. III-A (limited memory, real-time constraints, and energy constraints) while not sacrificing and often improving accuracy performance.

E. Parameter Study

We performed a series of parameter studies to assess the impact of different hyperparameters in MIMONet. In Fig. 4, we show the changes in compression ratio, training loss, and VIB loss during the training process. We observed that a decrease in the IB learning rate from $1e-1$ to $1e-5$ resulted in a slower increase in compression rate, as well as a slower decrease in training and VIB loss.

In Fig.5, we present scatterplots of accuracy and compression rate for different hyperparameters in MIMONet. We found that the IB learning rate parameter requires careful selection, with $1e-3$ being optimal for this study. For the KL parameter, a lower value setting (less than or equal to $1e-7$) produced models with high accuracy but less compression rate, while higher values resulted in higher compression rates but very low accuracy. Therefore, a value of $1e-7$ was optimal for the KL parameter in this study. Additionally, we investigated the impact of the merge degree hyperparameter on MIMONet [21], and found that it is insensitive to hyperparameters, with nearly lossless compression in all

cases. The learnable parameter number linearly decreases with an increase in the merge degree, and model accuracy ranges from 74.21% to 75.80%, with model accuracy after finetuning ranging from 75.12% to 76.67% (baseline MIMO model accuracy is 74.26%).

F. Case study on TurtleBot3

We conduct a case study using the TurtleBot3 robot to evaluate the real-world applicability of MIMONet. Specifically, we replace the TurtleBot3’s main control device with a Jetson Nano and install an RGB camera, USB audio card, and speakers. Subsequently, a native speaker was invited to converse with the robot using happy tones while facial videos were captured. The robot will make sounds and specific movements based on the predictions. We evaluate three models (MISO, baseline MIMO, and MIMONet) and find that MISO generated wrong results and exhibited the longest response time due to two-pass inferences. In contrast, baseline MIMO and MIMONet both yield accurate results, while MIMONet yields significantly shorter response times (3.00x speedup than baseline MIMO on average), which aligns with our evaluation (Sec. IV-C and Sec. IV-D).

G. Limitations and Discussion on Future Directions

Recent works on model compression have primarily focused on feed-forward models, while ResNet [12], Transformer [6], and GNNs [36, 37, 38] are more complex network structures that have received less attention. To enable the deployment of state-of-the-art models like BEiT-3 and Gato on on-device scenarios, we intend to explore the application of MIMONet to these more recent complex network structures. BEiT-3 [5] and Gato [7] do not currently consider on-device constraints and lack techniques that optimize latency, energy, and memory. Furthermore, while CPU-based embedded devices can benefit from our proposed approach, many AI-oriented embedded devices also have functional computing devices like FPGAs, TPUs, and NPUs that can be utilized to form heterogeneous systems on SoCs. We believe that optimizing the compression strategy considering the different characteristics of heterogeneous computing devices is a promising future direction for enabling on-device deployment for more general embedded devices.

V. CONCLUSION

This paper introduces MIMONet, one of the first on-device Multiple-Input Multiple-Output (MIMO) Deep Neural Network (DNN) frameworks targeting robotic applications. MIMONet achieves high accuracy and on-device efficiency in terms of critical performance metrics, such as latency, energy, and memory usage. Extensive experiments on three widely used embedded platforms demonstrate that MIMONet can provide high accuracy while enabling superior on-device efficiency, particularly when compared to state-of-the-art Single-Input Single-Output (SISO) and Multiple-Input Single-Output (MISO) models. Our research is an important first step toward building efficient MIMO DNN frameworks for practical on-device learning scenarios, particularly for robots that often face hardware and performance constraints.

REFERENCES

- [1] X. Deng, Y. Xiang, A. Mousavian, C. Eppner, T. Bretl, and D. Fox, "Self-supervised 6d object pose estimation for robot manipulation," in *2020 IEEE International Conference on Robotics and Automation (ICRA)*. IEEE, 2020, pp. 3665–3671.
- [2] X. Meng, N. Ratliff, Y. Xiang, and D. Fox, "Neural autonomous navigation with riemannian motion policy," in *2019 International Conference on Robotics and Automation (ICRA)*. IEEE, 2019, pp. 8860–8866.
- [3] Z. Yang, A. B. Clark, D. Chappell, and N. Rojas, "Instinctive real-time semg-based control of prosthetic hand with reduced data acquisition and embedded deep learning training," in *2022 International Conference on Robotics and Automation (ICRA)*. IEEE, 2022, pp. 5666–5672.
- [4] S. Su, Y. Li, S. He, S. Han, C. Feng, C. Ding, and F. Miao, "Uncertainty quantification of collaborative detection for self-driving," *arXiv preprint arXiv:2209.08162*, 2022.
- [5] W. Wang, H. Bao, L. Dong, J. Bjorck, Z. Peng, Q. Liu, K. Aggarwal, O. K. Mohammed, S. Singhal, S. Som, and F. Wei, "Image as a foreign language: Beit pretraining for all vision and vision-language tasks," *CoRR*, vol. abs/2208.10442, 2022. [Online]. Available: <https://doi.org/10.48550/arXiv.2208.10442>
- [6] A. Vaswani, N. Shazeer, N. Parmar, J. Uszkoreit, L. Jones, A. N. Gomez, L. Kaiser, and I. Polosukhin, "Attention is all you need," in *Advances in Neural Information Processing Systems 30: Annual Conference on Neural Information Processing Systems 2017, December 4-9, 2017, Long Beach, CA, USA*, I. Guyon, U. von Luxburg, S. Bengio, H. M. Wallach, R. Fergus, S. V. N. Vishwanathan, and R. Garnett, Eds., 2017, pp. 5998–6008. [Online]. Available: <https://proceedings.neurips.cc/paper/2017/hash/3f5ee243547dee91fbd053c1c4a845aa-Abstract.html>
- [7] S. E. Reed, K. Zolna, E. Parisotto, S. G. Colmenarejo, A. Novikov, G. Barth-Maron, M. Gimenez, Y. Sulsky, J. Kay, J. T. Springenberg, T. Eccles, L. Bruce, A. Razavi, A. Edwards, N. Heess, Y. Chen, R. Hadsell, O. Vinyals, M. Bordbar, and N. de Freitas, "A generalist agent," *CoRR*, vol. abs/2205.06175, 2022. [Online]. Available: <https://doi.org/10.48550/arXiv.2205.06175>
- [8] R. Hu and A. Singh, "Unit: Multimodal multitask learning with a unified transformer," in *2021 IEEE/CVF International Conference on Computer Vision, ICCV 2021, Montreal, QC, Canada, October 10-17, 2021*. IEEE, 2021, pp. 1419–1429. [Online]. Available: <https://doi.org/10.1109/ICCV48922.2021.00147>
- [9] Digitaldreamlabs, "Vector 2.0 ai robot companion," <https://www.digitaldreamlabs.com/products/vector-robot>, 2022.
- [10] B. Dai, C. Zhu, B. Guo, and D. Wipf, "Compressing neural networks using the variational information bottleneck," in *International Conference on Machine Learning*. PMLR, 2018, pp. 1135–1144.
- [11] G. Bebis and M. Georgiopoulos, "Feed-forward neural networks," *IEEE Potentials*, vol. 13, no. 4, pp. 27–31, 1994.
- [12] K. He, X. Zhang, S. Ren, and J. Sun, "Deep residual learning for image recognition," in *Proceedings of the IEEE conference on computer vision and pattern recognition*, 2016, pp. 770–778.
- [13] S. R. Livingstone and F. A. Russo, "The ryerson audio-visual database of emotional speech and song (ravdess): A dynamic, multimodal set of facial and vocal expressions in north american english," *PloS one*, vol. 13, no. 5, p. e0196391, 2018.
- [14] J. Guo, A. Li, and C. Liu, "Backdoor detection and mitigation in competitive reinforcement learning," 2023.
- [15] NVIDIA, "Duckiebot (db-j)," <https://get.duckietown.com/products/duckiebot-db21>, 2022.
- [16] —, "Sparkfun jetbot ai kit," <https://www.sparkfun.com/products/18486>, 2022.
- [17] —, "Waveshare jetbot ai kit," <https://www.amazon.com/Waveshare-JetBot-AI-Kit-Accessories/dp/B07V8JL4TF>, 2022.
- [18] Y. Hu, J. Yang, L. Chen, K. Li, C. Sima, X. Zhu, S. Chai, S. Du, T. Lin, W. Wang, et al., "Goal-oriented autonomous driving," *arXiv preprint arXiv:2212.10156*, 2022.
- [19] Z. Liu, H. Tang, A. Amini, X. Yang, H. Mao, D. Rus, and S. Han, "Bevfusion: Multi-task multi-sensor fusion with unified bird's-eye view representation," *arXiv preprint arXiv:2205.13542*, 2022.
- [20] L. Deng, G. Li, S. Han, L. Shi, and Y. Xie, "Model compression and hardware acceleration for neural networks: a comprehensive survey," *Proceedings of the IEEE*, vol. 108, no. 4, pp. 485–532, 2020.
- [21] X. He, Z. Zhou, and L. Thiele, "Multi-task zipping via layer-wise neuron sharing," in *Advances in Neural Information Processing Systems*, 2018, pp. 6019–6029.
- [22] X. Dong, S. Chen, and S. Pan, "Learning to prune deep neural networks via layer-wise optimal brain surgeon," in *Advances in Neural Information Processing Systems*, 2017, pp. 4860–4874.
- [23] B. Hassibi and D. G. Stork, "Second order derivatives for network pruning: Optimal brain surgeon," in *Advances in Neural Information Processing Systems*, 1993, pp. 164–171.
- [24] S. Liu, J. Du, K. Nan, Z. Zhou, H. Liu, Z. Wang, and Y. Lin, "Adadeep: A usage-driven, automated deep model compression framework for enabling ubiquitous intelligent mobiles," *IEEE Transactions on Mobile Computing*, pp. 1–1, 2020.
- [25] M. Courbariaux, Y. Bengio, and J.-P. David, "Binaryconnect: Training deep neural networks with binary weights during propagations," in *Advances in Neural Information Processing Systems*, 2015, pp. 3123–3131.
- [26] P. Molchanov, A. Mallya, S. Tyree, I. Frosio, and J. Kautz, "Importance estimation for neural network pruning," in *Proceedings of IEEE/CVF Conference on Computer Vision and Pattern Recognition*, 2019, pp. 11 264–11 272.
- [27] X. He, D. Gao, Z. Zhou, Y. Tong, and L. Thiele, "Pruning-aware merging for efficient multitask inference," in *Proceedings of ACM SIGKDD Conference on Knowledge Discovery & Data Mining*. New York, NY, USA: ACM, 2021, pp. 585–595.
- [28] Y.-M. Chou, Y.-M. Chan, J.-H. Lee, C.-Y. Chiu, and C.-S. Chen, "Unifying and merging well-trained deep neural networks for inference stage," in *Proceedings of International Joint Conference on Artificial Intelligence*, 2018, pp. 2049–2056.
- [29] H. Zhou, W. Li, Z. Kong, J. Guo, Y. Zhang, B. Yu, L. Zhang, and C. Liu, "Deepbillboard: Systematic physical-world testing of autonomous driving systems," in *Proceedings of the ACM/IEEE 42nd International Conference on Software Engineering*.
- [30] Z. Kong, J. Guo, A. Li, and C. Liu, "Physgan: Generating physical-world-resilient adversarial examples for autonomous driving," 2019.
- [31] K. Simonyan and A. Zisserman, "Very deep convolutional networks for large-scale image recognition," *arXiv preprint arXiv:1409.1556*, 2014.
- [32] X. He, X. Wang, Z. Zhou, J. Wu, Z. Yang, and L. Thiele, "On-device deep multi-task inference via multi-task zipping," *IEEE Transactions on Mobile Computing*, 2021.
- [33] D. P. Kingma and J. Ba, "Adam: A method for stochastic optimization," *arXiv preprint arXiv:1412.6980*, 2014.
- [34] A. Paszke, S. Gross, F. Massa, A. Lerer, J. Bradbury, G. Chanan, T. Killeen, Z. Lin, N. Gimeshin, L. Antiga, et al., "Pytorch: An imperative style, high-performance deep learning library," *Advances in neural information processing systems*, vol. 32, 2019.
- [35] NVIDIA, "tegrastats utility," https://docs.nvidia.com/drive/drive_os_5.1.6.1L/nvlib_docs/index.html#page/DRIVE.OS.Linux.SDK_Development_Guide/Utilities/util_tegrastats.html, 2022.
- [36] T. N. Kipf and M. Welling, "Semi-supervised classification with graph convolutional networks," in *5th International Conference on Learning Representations, ICLR 2017, Toulon, France, April 24-26, 2017, Conference Track Proceedings*. OpenReview.net, 2017. [Online]. Available: <https://openreview.net/forum?id=SJU4ayYgl>
- [37] W. L. Hamilton, Z. Ying, and J. Leskovec, "Inductive representation learning on large graphs," in *Advances in Neural Information Processing Systems 30: Annual Conference on Neural Information Processing Systems 2017, December 4-9, 2017, Long Beach, CA, USA*, I. Guyon, U. von Luxburg, S. Bengio, H. M. Wallach, R. Fergus, S. V. N. Vishwanathan, and R. Garnett, Eds., 2017, pp. 1024–1034. [Online]. Available: <https://proceedings.neurips.cc/paper/2017/hash/5dd9db5e033da9c6f55ba83c7a7e9-Abstract.html>
- [38] P. Velickovic, G. Cucurull, A. Casanova, A. Romero, P. Liò, and Y. Bengio, "Graph attention networks," in *6th International Conference on Learning Representations, ICLR 2018, Vancouver, BC, Canada, April 30 - May 3, 2018, Conference Track Proceedings*. OpenReview.net, 2018. [Online]. Available: <https://openreview.net/forum?id=rJXMPikCZ>